

This is a repository copy of *Biomass composition of the golden tide pelagic seaweeds Sargassum fluitans and S. natans (morphotypes I and VIII) to inform valorisation pathways*.

White Rose Research Online URL for this paper:

<https://eprints.whiterose.ac.uk/166848/>

Version: Accepted Version

Article:

Davis, Doleasha, Simister, Rachael, Campbell, Sanjay et al. (6 more authors) (2021) Biomass composition of the golden tide pelagic seaweeds Sargassum fluitans and S. natans (morphotypes I and VIII) to inform valorisation pathways. Science of the Total Environment. 143134. ISSN 0048-9697

<https://doi.org/10.1016/j.scitotenv.2020.143134>

Reuse

This article is distributed under the terms of the Creative Commons Attribution-NonCommercial-NoDerivs (CC BY-NC-ND) licence. This licence only allows you to download this work and share it with others as long as you credit the authors, but you can't change the article in any way or use it commercially. More information and the full terms of the licence here: <https://creativecommons.org/licenses/>

Takedown

If you consider content in White Rose Research Online to be in breach of UK law, please notify us by emailing eprints@whiterose.ac.uk including the URL of the record and the reason for the withdrawal request.

Biomass composition of the golden tide pelagic seaweeds *Sargassum fluitans* and *S. natans* (morphotypes I and VIII) to inform valorisation pathways.

Doleasha Davis^{a,b*}, Rachael Simister^{b*}, Sanjay Campbell^{a,b}, Melissa Marston^a, Suranjana Bose^c
Simon J. McQueen-Mason^b, Leonardo D. Gomez^b, Winklet A. Gallimore^a, and Thierry Tonon^{b#}.

^a Department of Chemistry, University of the West Indies, Mona Campus, Mona, Kingston 7, Jamaica.

^b Department of Biology, Centre for Novel Agricultural Products, University of York, Heslington, York YO10 5DD, United Kingdom.

^c Green Chemistry Centre of Excellence, Department of Chemistry, University of York, Heslington, York YO10 5DD, United Kingdom.

* Equal contribution.

Corresponding author: thierry.tonon@york.ac.uk

Abstract

Massive strandings of the pelagic brown algae *Sargassum* have occurred in the Caribbean, and to a lesser extent, in western Africa, almost every year since 2011. These events have major environmental, health, and economic impacts in the affected countries. Once on the shore, *Sargassum* is mechanically harvested and disposed of in landfills. Existing commercial applications of other brown algae indicate that the pelagic *Sargassum* could constitute a valuable feedstock for potential valorisation. However, limited data on the composition of this *Sargassum* biomass was available to inform on possible application through pyrolysis or enzymatic fractionation of this feedstock. To fill this gap, we conducted a detailed comparative biochemical and elemental analysis of three pelagic *Sargassum* morphotypes identified so far as forming Atlantic blooms: *Sargassum natans* I (SnI), *S. fluitans* III (Sf), and *S. natans* VIII (SnVIII). Our results showed that SnVIII accumulated a lower quantity of metals and metalloids compared to SnI and Sf, but it contained higher amounts of phenolics and non-cellulosic polysaccharides. SnVIII also had more of the carbon storage compound mannitol. No differences in the

content and composition of the cell wall polysaccharide alginate were identified among the three morphotypes. In addition, enzymatic saccharification of SnI produced more sugars compared to SnVIII and Sf. Due to high content of arsenic, the use of pelagic *Sargassum* is not recommended for nutritional purposes. In addition, low yields of alginate extracted from this biomass, compared with brown algae used for industrial production, limit its use as viable source of commercial alginates. Further work is needed to establish routes for future valorisation of pelagic *Sargassum* biomass.

Keywords

Sargassum; the Caribbean; western African; composition analysis; biomass valorisation; seaweed strandings.

1. Introduction

Sargassum fluitans and *S. natans* are species of surface dwelling (pelagic) brown seaweeds that have inundated the shores of the Caribbean, and, to a lesser extent, the western African shoreline, since 2011 (Smetacek and Zingone, 2013; Langin, 2018; Milledge et al., 2020). Large populations of *Sargassum* have proliferated almost every year since then, forming what Wang et al. (2019) described as the “Great Atlantic *Sargassum* Belt (GASB)”. This GASB was estimated to be 8,850 km long and to contain over 20 million metric tons of biomass in June 2018. Such massive inundation events are known as golden tides due to the golden brown colour of *Sargassum*. These seaweeds threaten coastal environments because they begin to rot shortly after reaching shallow waters and beaches, removing oxygen from the surrounding water, killing fish and other marine organisms. *Sargassum* also raises human health concerns due to large amounts of toxic gases, including hydrogen sulphide and ammonia, are produced when the seaweeds start decomposing on the seashore (Resiere et al., 2018). Exposure to high concentrations of hydrogen sulphide can lead to pulmonary, neurological, and cardiovascular lesions. In addition, *Sargassum* has negative impacts on the fishing and tourism industries in the Caribbean, as well as in western Africa (Adet et al., 2017; Ofori et al. 2020).

Once on the beach, *Sargassum* is mechanically harvested and brought to a landfill. *Sargassum* clean-up costs for the Caribbean region were estimated at USD \$210 million for the year 2018 by the Caribbean Regional Fisheries Mechanism, causing severe impacts on local economies, and highlighting the need for more information on the massive stranding events. At present, efforts to forecast and estimate biomass volumes are based mainly on the analysis of satellite data (Ody et al., 2019; Wang et al., 2019). Seaweeds causing these massive algal blooms in the Atlantic have been identified as being *S. fluitans* III (Sf), *S. natans* I (SnI), and *S. natans* VIII (SnVIII) morphotypes (Schell et al., 2015; Amaral-Zettler et al., 2017; Govindarajan et al., 2019). Recent reports suggest a combination of factors, including winds, currents and sources of nutrients, to explain the establishment, and recurrence, of pelagic *Sargassum* blooms (Putman et al., 2018; Oviatt et al., 2019; Wang et al., 2019; Johns et al., 2020).

Sargassum seaweeds are very abundant in tropical and subtropical regions, forming large floating rafts and inhabiting rocky reefs. Because these algae account for large biomass, Gouvêa et al.

(2020) suggested their contribution is relevant for global carbon stocks and consequently for mitigating climate change as CO₂ remover. There is also interest in exploiting the bioremediation potential of *Sargassum* sp. to tackle pollution in coastal environments (Saldariagga- Hernandez et al., 2020). Brown seaweeds are harvested from wild populations or farmed to provide valuable products, including texturing agents for the food industry, biofuels, fertilisers, animal feed, nutraceuticals, and cosmeceuticals (Kraan, 2013). A biorefinery approach, valorising different fractions of the biomass, has been put forward for *S. muticum* to obtain high value/low volume and high volume/low value products (Balboa et al., 2015; Milledge et al., 2016; Pérez-Larrán et al., 2019). The prospect for valorisation of *S. fluitans* and *S. natans* biomass has not been unnoticed, and Milledge and Harvey (2016) have reviewed the potential uses and obstacles for exploitation of pelagic *Sargassum*. In line with this, Thompson et al. (2020) have recently investigated the feasibility of using this biomass as a feedstock for the production of fertiliser and electricity in Barbados, one of the Caribbean nations affected by golden tides. However, considering results obtained by Milledge et al. (2020), exploitation of pelagic *Sargassum* biomass alone for the production of biogas may be challenging because of the limited production of methane from such feedstock.

The exploitation of seaweed biomass and definition of valorisation pathways should be informed by thorough knowledge of the biomass composition. Previous compositional analysis of pelagic *Sargassum* collected outside the Sargasso Sea was conducted on mixtures of *S. natans* and *S. fluitans*. Samples from the Nigerian coast were used to determine crude protein, crude fat, fibre, moisture, ash, carbohydrate, minerals and phytochemical content (Oyesiku and Egunyomi, 2014). Biomass harvested along the coast of the western region of Ghana were analysed for nutritional (nitrogen, phosphate, ammonia, nitrate and potassium) and toxicological (copper, zinc, iron, lead, cadmium, mercury, arsenic and chloride) parameters (Addico and deGraft-Johnson, 2016). Algae collected from the Southern North Atlantic were considered for biochemical analysis (C: N ratio, fatty acids, and stable isotopes) (Baker et al., 2018). Sembera et al. (2018) assessed compost quality of *Sargassum* harvested from the shoreline of a Texas beach. Other studies have dealt with individual morphotypes. Rhein-Knudsen et al. (2017) and Mohammed et al. (2018, 2019) used *S. natans* from Ghana and Trinidad and Tobago respectively, and Rosado-Espinosa et al. (2020) *S. fluitans* from the

Yucatan coast (Mexico), for extraction and characterization of the cell wall polysaccharide alginate. More recently, Rodríguez-Martínez et al. (2020) described variations in the elemental concentrations between Sf, SnI and SnVIII harvested on the Mexican Caribbean coast. Milledge et al. (2020) investigated differences in methane potential related to moisture, ash, salt, carbon, hydrogen, nitrogen, sulphur, phenolic, lipid, amino acid, metal and metalloid contents among the three pelagic morphotypes collected from the Caribbean islands of Turks and Caicos. However, no information such as pyrolysis analysis, content of the antioxidant phlorotannins, and quantification of individual monosaccharides were available to define pathways for valorisation. In addition, data was missing on the potential to fractionate *Sargassum* biomass using enzymes.

In this context, the main objectives of our study were to produce an in-depth characterisation of the pelagic *Sargassum* morphotypes, and to investigate the influence of enzymes to facilitate biomass fractionation, to inform pathways for the valorisation of this seaweed biomass and the benefits of affected countries. To this aim, we report a detailed comparative biochemical and elemental characterization, and the monosaccharide profiles obtained after enzymatic treatments, of the individual Sf, SnI, and SnVIII morphotypes, and of a bulk mixture (containing mostly Sf) collected from the south coast region of Jamaica in February 2019. Our results point to differences between morphotypes and establish a compositional library that will contribute to define possible valorisation routes for pelagic *Sargassum* biomass.

2. Materials and Methods

2.1. Study sites, field collection, and preparation of seaweed samples

Sargassum biomass was collected on the 6th of February 2019 from three different sites in the vicinity of Port Royal, Jamaica. These sites were labelled for analysis purposes as follows: Site A, Fort Rocky (17°56'12.0"N 76°49'08.4"W); Site B, Port Royal (17°56'09.2"N 76°50'17.2"W); site C, Lime Cay (17°55'06.1"N 76°49'12.8"W) (Figure 1A). Wet algae were manually collected fresh from inshore water, before they reached the shore and begun to dry. After harvesting, algae were bagged and brought

to the laboratory the same day of collection. After washing with tap water to remove natural solid contaminants, biomass from each of the three sampling sites was separated into three different morphotypes according to criteria previously described (Schell et al., 2015; Amaral-Zettler et al., 2017): *S. fluitans* III (Sf), *S. natans* I (SnI), and *S. natans* VIII (SnVIII) (Figure 1B). A bulk sample of unprocessed algae (Sfm), observed to be composed mainly of Sf (estimated by visual observation to be 10 times more than the *S. natans* biomass), was also considered for the three sites as it represents raw biomass that could be used for subsequent processing without any prior separation. The resulting twelve samples were kept for two days in the freezer, before drying at University of the West Indies, Mona Campus (Jamaica). For this, samples were placed on drying trays, exposed in direct sunlight during the days for approximately 6-8 hours daily (estimated temperatures of 29 - 31 °C), and frequently rotated to ensure thorough drying. They were stored at room temperature during the nights of the three days of the drying for the morphotype samples, and of the seven days for the bulk samples (longer process due to difference in volume of samples). After drying, approximately half of the dried biomass for each sample was sent to York (UK), where it was milled for 50 sec at 300 MHz with a tissueLyser II (Qiagen) using a 20 mm stainless steel grinding ball in a 10 ml grinding jar (Qiagen).

2.2. Thermogravimetric analysis

Seaweed samples and calcium carbonate powder (Sigma) were analysed using a NETZSCH STA 409 instrument. The heating rate was controlled at 10 °C min⁻¹ from 25 to 800 °C. Nitrogen was used as the carrier gas at a flow rate of 100 ml/min.

2.3. Analysis of elemental composition by inductively coupled plasma mass spectrometry (ICP-MS)

Three technical replicates were prepared for the three morphotypes collected at site A. Approximately 0.2 g of sample was weighed accurately into a digestion vessel, and 8 ml of concentrated HNO₃ and 2 ml of 30% H₂O₂ were added. The digestion vessels were sealed and placed into a microwave (Milestone Ethos Up). A thermocouple was placed into the first digestion vessel to monitor the temperature of the liquid inside. The microwave was programmed to heat the contents of the digestion vessels to 200 °C over a period of 30 min. Once at the desired temperature, contents were

kept at 200 °C for a period of 15 min. After this, the digestion vessels were cooled down before diluting to 100 ml with distilled water. Ten ml of each sample were used for subsequent analysis. An environmental stock calibration fluid (ICP-MS calibration, Agilent part number 5183-4688), with a known concentration of many common elements found in the environment, was used to produce low (Ag, Al, As, Ba, Be, Cd, Co, Cr, Cu, Mn, Mo, Ni, Pb, Sb, Se, Th, Tl, U, V, Zn: 10,000 ppb) and high (Ca, Fe, K, Mg, Na: 1,000,000 ppb) concentration calibration standards. Algal samples and calibration solutions were run on an Agilent 7700x ICP-MS equipped with a helium collision cell.

2.4. Quantification of phenolic and phlorotannin contents

For each sample, 0.25 g of dried algal powder was loaded into a glass flask. Acetone-H₂O mixture (70% /30 % v/v, 17.5 ml) was added, and the flasks were covered with aluminium foil for extraction at room temperature in the dark for 24 h. The extracts were centrifuged at 4,000 rpm at 4°C for 8 min, and the supernatants concentrated by evaporation using a rotary evaporator. The dried extracts were thereafter re-suspended in 3-4 ml of methanol.

The phenolic content in each sample was determined by the Folin-Ciocalteu (FC) method (Singleton et al., 1999), using phloroglucinol methanolic solutions (0-0.250 mg/ml) as standards. The methanolic extract of the brown algae (100 µl) was mixed with 800 µl of the 10% 2N FC reagent, and 800 µl of 1M Na₂CO₃ were added. The resulting mixture was incubated at 40 °C for 15 min and then at room temperature for one hour. Post incubation, the absorbance was read at 650 nm on a Sunrise microplate reader spectrophotometer (Tecan) and phenolic contents were expressed as phloroglucinol equivalents (PGE) in mg/g of biomass dried weight (DW).

The phlorotannin content of each fraction was determined by the 2,4-dimethoxybenzaldehyde (DMBA) assay, which reacts specifically with m-diphenolics (1,3- and 1,3,5-substituted phenols), and is more specific than the FC reagent that reacts also with mono- and o-diphenolics (Stern et al., 1996). Phloroglucinol (0-0.06 mg/ml) methanolic solutions were used as standards. An aliquot of the methanolic solution of the dry extract (50 µl) was mixed in a capped tube with 50 µl of MeOH and 1.5 ml of working solution. This solution was obtained by mixing equal volumes of DMBA (3%, m/v) and HCl (3%, v/v), both prepared in glacial acetic acid and mixed prior to use. Samples were incubated for

one hour at room temperature in the dark. The absorbance was read at 515 nm on a visible spectrophotometer (Varian 50 Bio), and the concentrations of the phlorotannins were expressed as phloroglucinol equivalents (PGE) in mg/g of algal biomass DW.

2.5. Determination of monosaccharide composition of the non-cellulosic fraction of the biomass

Approximately five mg of each sample were weighed in triplicate in screw capped tubes. Samples were partially hydrolysed by adding 0.5 ml of 2 M trifluoroacetic acid (TFA). The vials were flushed with dry argon, mixed and heated at 100 °C for four hours, mixing periodically. The vials were then cooled to room temperature and dried in a centrifugal evaporator with fume extraction. Five hundred µl of 2-propanol were added to the samples, and vortexed before drying in centrifugal evaporator. This was then repeated once. Finally, the samples were resuspended in 200 µl of deionised water, mixed, centrifuged at 11,600 rpm for 5 min. The supernatant was filtered with 0.45 µm PTFE filters into HPLC vials, and analysed by high-performance anion-exchange chromatography on a Dionex Carbopac PA-10 column using integrated amperometry detection as described in Jones et al. (2003). To enable quantification, a standard sugar mixture containing arabinose, fucose, galactose, glucose, mannose, rhamnose, xylose, galacturonic acid, glucuronic acid, guluronic acid, mannuronic acid, and mannitol, was prepared and treated as indicated above for algal samples.

2.6. Production of alcohol insoluble residues (AIRs)

Sn I site C, Sf site C, and Sn VIII site B were selected because they represented the samples with the largest amounts of biomass available for each morphotype. Approximately half of the dried biomass from each sample was weighed, and the accurate mass recorded to calculate the % of soluble material). *Sargassum* powder was mixed with 75% ethanol, placed in boiling bath for 5 min, and span down for 5 min at room temperature. The supernatants were discarded, and pellets used to repeat wash with 75% ethanol twice. After this, a fourth wash was done with 96% ethanol under identical conditions. The resulting pellets were then washed in acetone, dried at 50 °C for 2 days, and weighed. The dried samples were kept for enzyme digestion analysis.

2.7. Enzymatic digestion

AIRs were used for enzymatic digestions with enzyme at 1 mg/ml final concentration, or in absence of enzyme, replaced by buffer, as control. All samples were incubated for 24 hours at the indicated optimum temperature for each enzyme: (1) 50 mg of biomass were re-suspended in 1.5 ml of 25 mM Na Acetate Buffer pH 4.5, and 215 µl of Cellic2® CTec2 (Novozymes) added before incubation at 50 °C; (2) 50 mg of biomass were re-suspended in 1.5 ml of 10 mM potassium phosphate buffer, pH 6.5, 1 mM CaCl₂, 0.05% NaN₃, and 150 µl of amyloglucosidase (Sigma) added before incubation at 25 °C; (3) 50 mg of biomass were re-suspended in 1.5 ml of 100 mM potassium phosphate buffer pH 7, and 100 µl of pronase (Roche) added before incubation at 40 °C; (4) 50 mg of biomass were re-suspended in 1.5 ml of laminarinase buffer pH 6.2 (HEPES 50 mM, NaCl 25 mM, CaCl₂ 3.5 mM), and 50 µl of laminarinase (NZYTech, Portugal) added before incubation at 90 °C; (5) 50 mg of biomass were re-suspended in 1.5 ml of alginate lyase buffer pH 9 (HEPES 50 mM, NaCl 25mM, CaCl₂ 3.5 mM), and 50 µl of alginate lyase (NZYTech, Portugal) added before incubation at 30 °C. After digestion, samples were centrifuged for five minutes at 13,000 rpm, 100 µl of the supernatant was dried down, and 0.5 ml of 2 M TFA was added for monosaccharide composition analysis as described in section 2.5.

2.8. Data analysis

To assess potential differences in the biochemical and elemental composition between the three pelagic *Sargassum* morphotypes, statistical analysis was conducted using SigmaPlot version 14.0. For thermogravimetric analysis, as well as for comparison of monosaccharide composition, and of phenolic and phlorotannin contents, values for samples corresponding to the same morphotype, or to the bulk, and harvested at the three sites of collection, were pooled together. However, bulk values were not considered for the statistical tests to focus on comparison between the three morphotypes. Data were first tested for normality and homogeneity of variance using the Shapiro-Wilk test and Brown-Forsythe test, respectively. When these tests were passed, one-way ANOVA was performed, followed by a post-hoc Holm-Sidak test for all pairwise multiple comparisons. When the normality test (Shapiro-Wilk) failed, Kruskal-Wallis one-way analysis of variance on ranks was applied, followed by a post hoc Tukey

test for all pairwise multiple comparisons. In addition, T-test done in Excel was used to assess the impact of enzymatic treatment on monosaccharide composition of alcohol insoluble residues. The significance level was set at $p\text{-value} \leq 0.05$ for all the data analysis.

3. Results and Discussion

3.1. Thermogravimetric (TG) analysis of *S. natans* and *S. fluitans* morphotypes

The first weight loss in the TG profiles corresponded to evaporation of water at 100 °C, and the moisture content represented approximately 7-8 weight % in the three morphotypes and the bulk sample, with no significant differences between Sf, SnI, and SnVIII (Figure 2, and Supplementary Table S1). After the start of pyrolysis, i.e. once vaporization of all moisture has happened, the main weight loss was observed between 200 and 400 °C. Based on previous analysis of different brown algal biomass (Ross et al., 2009; Bae et al., 2011; Kim et al., 2012 and 2013), and of polysaccharides and carbohydrates of these organisms (Anastasakis et al., 2011), this can be attributed to the decomposition of carbohydrates (between 200-300 °C) and of proteins (300-400 °C). These mass losses ranged between 28.86 ± 0.40 (Sf) and 33.73 ± 1.47 (SnVIII) weight %, with significant differences observed between SnVIII and Sf ($p = 0.017$), and SnVIII and SnI ($p = 0.015$). A third mass loss step was identified in most of the samples, occurring from 600 °C, and was suggested to be due to calcium carbonate, i.e. the mineral part of the exoskeleton of encrusting bryozoan. Indeed, variable quantities of white material in the dried *Sargassum* samples before analysis were observed, and the occurrence of bryozoans on the surface of pelagic *Sargassum* has been previously reported in the literature (Weis, 1968; Taylor and Monks, 1997). We confirmed the presence of calcium carbonate in the algal samples by analysing in parallel calcium carbonate standard powder. Calcium carbonate accounted for 6.30 ± 0.47 (SnVIII) to 10.75 ± 1.10 (Sf) weight %, with a significant difference only between SnVIII and Sf ($p = 0.032$).

When thermal decomposition was carried out up to 800 °C to assess pyrolysis of pelagic *Sargassum* samples, the content of char ranged between 35.16 ± 6.05 (SnI) and 39.63 ± 1.34 (Sf) weight %, without any significant differences between the three morphotypes. It was slightly below (34.12 ± 3.46) in the bulk samples (Figure 2). Such values were in the lower range compared to those measured

by TG analysis of *Sargassum* sp. from Vietnam (average of 46.17 weight %; Kim et al., 2013) or from the Red Sea (46.15 weight %; Ali and Bahadar, 2017). One potential use of the char produced by pyrolysis from pelagic *Sargassum* could be as soil enhancer, as previously suggested for other seaweeds (Bird and Benson, 1987), including *Sargassum* sp. (Roberts et al., 2015). This possible route for valorisation was discussed in details by Milledge and Harvey (2016), who indicated that the use of solar drying prior to pyrolysis for biochar production could potentially balance the insufficient energy within the *Sargassum* feedstock for drying. However, the high concentration of salt, and the accumulation by pelagic *Sargassum* morphotypes of high level of toxic elements, e.g. arsenic, should be considered cautiously.

3.2. Determination of the elemental composition of pelagic *Sargassum* morphotypes

For this analysis, samples collected from site A were used, and eighteen elements were quantified, representing about 10% of the biomass DW (Table 1). The total amounts determined were similar between SnI and Sf, while being statistically different, and lower, for SnVIII (SnVIII vs. SnI: $p = 0.004$; SnVIII vs. Sf: $p = 0.002$; Supplementary Table S2). Significant variations were observed for the macroelements Na, Mg, and Ca (all p -values ≤ 0.001 for SnVIII vs. SnI and SnVIII vs. Sf). For the microelements, amounts of Fe and Mn were significantly different among the three morphotypes (all p -values ≤ 0.05). Among metalloids, arsenic content was significantly higher in SnI ($64.91 \pm 0.61 \mu\text{g/g DW}$), compared with SnVIII ($60.30 \pm 0.34 \mu\text{g/g DW}$; $p = 0.031$) and Sf ($58.32 \pm 2.29 \mu\text{g/g DW}$; $p = 0.009$). These values were in the wide range of levels previously reported for *Sargassum* species (20–231 $\mu\text{g/g DW}$; Milledge et al., 2016). However, they are higher than those determined by Milledge et al. (2020) from the same three morphotypes collected in Turks and Caicos (Atlantic Ocean) (21–30 $\mu\text{g/g DW}$). Arsenic contents measured in Jamaican samples were above the maximum level permitted for seaweed meal and feed materials derived from seaweed in Europe (40 $\mu\text{g/g DW}$; Official Journal of the European Union, 2019), and exceeded limits recommended for agricultural soils in different countries (15–50 $\mu\text{g/g DW}$; Rodríguez-Martínez et al., 2020). This has been previously observed in *S. fluitans* and *S. natans* biomass harvested in Nigeria (Oyesiku and Egunyomi, 2014), Ghana (Addico and deGraft-Johnson, 2016), Dominican Republic (Fernández et al., 2017), and more recently for the three

pelagic *Sargassum* morphotypes collected along the Caribbean coast of Mexico (Rodríguez-Martínez et al., 2020). In this latter study, it was clearly suggested that the use of pelagic *Sargassum* for nutritional purposes should be avoided. In this context, the elemental concentration represents an important constraint to be taken into account when considering *S. fluitans* and *S. natans* for incorporation into animal feed and/or human diet, as well as for the production of compost and fertiliser. Importantly, organic and inorganic forms of metals and metalloids, such as for arsenic, are known to have varying degrees of toxicity (Gong et al. 2002); this underlines the need to investigate the speciation of these elements in *S. fluitans* and *S. natans* biomass before implementing valorisation pathways.

3.3. Determination of phenolic and phlorotannin content

After combining results from samples collected for each morphotype at the different collection sites, the phenolic content ranged between 1.20 ± 0.43 (Sf) and 3.11 ± 0.74 (SnVIII) mg/g of biomass DW. Phlorotannins are phloroglucinol-based phenolic compounds produced by brown macroalgae, and have been recognized for their bioactive properties and commercial potential (Ford et al., 2019). Their contents was comprised between 0.39 ± 0.21 (Sf) and 0.91 ± 0.32 (SnVIII) mg/g of biomass DW (Table 2). The values determined for the bulk samples were in the same ranges as those for Sf. These phenolic contents are similar to those determined by Milledge et al. (2020) in pelagic *Sargassum* collected in Turks and Caicos. The percentage (w/w) of phenolic compounds in the Jamaican samples ranged between 0.12-0.43 % of the biomass DW, and between 0.04 and 0.09 % of the biomass DW for the phlorotannins. These values were lower than those determined by Oyesiku and Egunyomi (2014), i.e. phenolics representing 0.8% of the biomass DW and tannins 1.22%, using a dried mixture of *S. natans* and *S. fluitans* collected in Nigeria and different analytical approaches.

When comparing the three morphotypes, significant variations in the phenolic content were observed between SnVIII and Sf ($p < 0.001$), and SnVIII and SnI ($p = 0.01$), but not between SnI and Sf (Supplementary Table S3). For the phlorotannins, the only statistically supported difference occurred between SnVIII and Sf ($p = 0.002$). In line with our results, Milledge et al. (2020), using the FC method, observed significant variations in the phenolic content between the three *Sargassum* morphotypes. These observations, based on seaweeds collected in very distant locations, support the fact that *S. natans*

and *S. fluitans* contains different levels of phenolic compounds. In the context of exploiting pelagic *Sargassum* biomass, it will be interesting to assess if there are seasonal changes in their phenolic and phlorotannin content, since such variations have been previously reported in *S. muticum* harvested in the Isle of Wight (Gorham and Lewey, 1984), and in western Brittany (Plouguerné et al., 2006). In addition, due to the increasingly recognised nutritional and health benefits of brown algal polyphenols (Fernando et al., 2016), it will be important to explore further the chemical structure and reactivity of pelagic *Sargassum* phlorotannins for possible use in nutraceuticals, functional foods, cosmetic, and pharmaceutical applications.

3.5. Analysis of the non-cellulosic fraction of pelagic *Sargassum* morphotypes.

The total monosaccharide content across the three morphotypes ranged between 142.76 ± 32.95 (Sf) and 183.94 ± 27.46 (SnVIII) μg of monosaccharides per mg biomass DW (Figure 3), and was found to be slightly higher in the bulk samples (193.98 ± 55.05). Statistical difference was only found between content in SnVIII and Sf ($p = 0.027$) (Supplementary Table S4).

The most abundant monosaccharides investigated were mannuronic (M) and guluronic (G) acids (65-67 % of the total monosaccharides, Table 3). These are the monomers forming alginate, the main brown algal cell wall polysaccharides, which represented 9-12 % of the morphotype DW. These values were in the lower range compared to alginate content determined for representative *Sargassum* species from different locations (9.3-49.9 % DW; Rosado-Espinosa et al. (2020). Guluronic and mannuronic acid accounted for 34-35 % and 65-66 % of the alginates respectively, with M/G ratios ranging from 1.87 ± 0.12 (SnI) to 1.97 ± 0.39 (SnVIII). No statistically supported differences were observed in the alginate content and the M/G ratio between the three morphotypes. Previous analysis using *S. natans* (no information given on the morphotype) harvested on the Ghanaian coast in January 2015 shown that alginate represented 30% of the seaweed biomass (Rhein-Knudsen et al., 2017), contained 53% of G and 32% of M, with an M/G ratio equal to 0.6. Differences in alginate content and composition observed between previous and current studies can be related to the distinct sites of collection (Gulf of Guinea and Caribbean Sea), to adaptation to changing growth conditions through the years, and the use of different experimental procedures. Lower yields of alginate observed in the

three pelagic *Sargassum* morphotypes (9-12%), compared to 12-45% from the brown seaweeds used for industrial production (Peteiro 2018), are likely to limit their use as a viable source of commercial alginate. This polysaccharide is one of the most versatile polymers, historically used in a wide ranges of industries (food, feed, textile printing, papermaking and pharmaceutical), and with more recent applications in the biomedical and bioengineering fields (Peteiro et al. 2018). Interestingly, recent work using *S. natans* harvested in the Caribbean suggested that sodium alginate extracted from this species could be used as an alternative for packaging and encapsulation (Mohammed et al. 2018), and calcium alginate could be considered as a successful biosorbent of heavy metals ions (Mohammed et al. 2019). These observations warrant further analysis of the structure and properties of alginates extracted from pelagic *Sargassum*.

Two other uronic acids were identified in pelagic *Sargassum* samples. Very low amounts of galacturonic acid were quantified, while glucuronic acid content ranged between 6.82 ± 2.00 (Sf) and 9.44 ± 1.58 $\mu\text{g}/\text{mg}$ of biomass DW (SnVIII). Significant variations were observed only for glucuronic acid between SnVIII and Sf ($p = 0.008$) (Supplementary Table S4).

Apart from uronic acids, the most abundant monosaccharide was fucose, accounting for 15.46 ± 1.47 (Sf) to 16.83 ± 0.94 (SnVIII) $\mu\text{g}/\text{mg}$ of biomass DW. Variations in its content were statistically supported only between Sf and SnVIII ($p = 0.046$). Fucose is the main precursor of the brown algal sulphated cell wall polysaccharides fucoidans and fucans (Deniaud-Bouët et al., 2014). Galactose corresponded to the second most abundant sugar quantified in the algal samples, ranging from 10.44 ± 2.44 (Sf) to 12.50 ± 0.81 (SnI) $\mu\text{g}/\text{mg}$ of biomass DW, and its content did not show significant variation when comparing the three morphotypes. Similar observations were made for glucose (from 4.25 ± 1.53 (Sf) to 4.92 ± 0.40 (SnI) $\mu\text{g}/\text{mg}$ of biomass DW), and xylose (from 4.19 ± 0.33 (SnI) to 4.61 ± 0.99 (SnVIII) $\mu\text{g}/\text{mg}$ of biomass DW). In contrast, quantities of mannose, from 3.53 ± 1.37 (Sf) to 4.82 ± 1.10 (SnVIII) $\mu\text{g}/\text{mg}$ of biomass DW, were significantly different between SnVIII and Sf ($p = 0.04$), as for fucose. Lower quantities of rhamnose (from 1.16 ± 0.43 (SnVIII) to 1.48 ± 0.31 (SnI) $\mu\text{g}/\text{mg}$ of biomass DW) and arabinose (from 1.13 ± 0.17 (SnI) to 1.19 ± 0.16 (Sf) $\mu\text{g}/\text{mg}$ of biomass DW) were determined, without any differences across three morphotypes. Higher content of fucose in SnI, SnVIII, and Sf compared to other sugars was not unexpected based on previous reports for *S. muticum*. Several

studies have described differential fractionation methods for valorisation of this seaweed, and analysis of sugar content (fucose, galactose, xylose, glucose and mannose) in extracts produced after different treatments shown that fucose was the most abundant sugar in the majority of the fractions obtained (Balboa et al., 2015; Álvarez-Viñas et al., 2019; Pérez-Larrán et al., 2019).

SnVIII contained approximately four times more mannitol than the other morphotypes, which content ranged from 1.77 ± 0.80 (Sf) to 7.24 ± 1.13 (SnVIII) $\mu\text{g}/\text{mg}$ of biomass DW. This represented less than 1% of the biomass DW of these algae. Differences in mannitol content were supported statistically between SnVIII and Sf, and SnVIII and SnI, with $p < 0.001$. Mannitol, one form of carbon storage used by brown algae, is therefore the only monosaccharide investigated for which significant changes were observed between the two *S. natans* morphotypes. In line with this, a great variability in the mannitol content has been reported within the genus *Sargassum* (1-34% biomass DW; Zubia et al., 2008), depending on season, site of collection, and species.

3.6. Production of alcohol insoluble residues (AIRs) and release of monosaccharides by different enzymatic treatments

AIRs were prepared, and mass loss between morphotypes was similar: 15.7% for SnI, 17.7% for Sf, and 22.4% for SnVIII (Supplementary Figure S1). This was within the range of soluble content observed in land plant biomass (Templeton et al., 2016). A study evaluating the potential of plant feedstock for sustainable production of biorenewables production showed soluble contents ranging between 3.39 and 28.29% of biomass (Lima et al., 2014). AIRs were subsequently used for individual enzymatic treatment using enzymes known to hydrolyse land plant cell walls (Cellic® CTec2) and starch (amyloglucosidase), brown seaweed cell wall component alginates (alginate lyase), and carbon storage polysaccharide (laminarinase), as well as a protease (pronase). The buffer only controls extracted a small amount of monosaccharides (Figure 4). This was not unexpected due to the length of the extraction and the high solubility of some compounds in macroalgae. Most of the enzymatic treatments released significantly higher amounts of monosaccharides compared to the control conditions, with the exception of Sf incubated in presence of alginate lyase and of SnVIII in presence of laminarinase (Supplementary Table S5). The highest amount of monosaccharides released after

hydrolysis was observed for SnI when compared with the other two morphotypes. The enzymes Cellic® Ctec2 and amyloglucosidase released the highest quantities of monosaccharides among the five enzymes tested and across all the samples investigated, while the enzymes acting on brown algal polysaccharides and pronase generally gave a lower yield, with the exception of SnI. Glucose, mannose, and galactose were the most abundant monosaccharides released through enzyme hydrolysis, mainly by the Cellic® Ctec2 and amyloglucosidase. The low efficiency of commercial laminarinase and alginate lyase may be due to a lack of specificity towards carbon storage and cell wall polysaccharides of the pelagic *Sargassum* biomass for which structure has not been characterised yet. In addition, it is anticipated that sequential enzyme combinations, with and without acid pre-treatment, will release a higher amount of monosaccharides from pelagic *Sargassum* for subsequent applications. Such experiments have been conducted using *Sargassum* sp. harvested in different countries. Borines et al. (2013) subjected *Sargassum* biomass harvested from Philippines to acid hydrolysis, and then to enzyme saccharification in the presence of cellulase and cellobiase for the production of ethanol. Similarly, Saravanan et al. (2018) reported ethanol production based on algal hydrolysate produced by acid and enzyme (cellulase and pectinase) treatment considering *Sargassum* from India. In the same vein, Azizi et al. (2017) considered *Sargassum* sp. from Persian Gulf for acid hydrolysis and enzyme saccharification (cellulase and cellobiase) to produce algal hydrolysate subsequently used for microbial production of polyhydroxyalkanoates, some of the most encouraging alternatives to conventional plastics. These examples pave the way for further experiments on enzymatic pre-treatments of pelagic *Sargassum* biomass for the production of ethanol and bioplastics, and may contribute to extend the portfolio of potential applications for this feedstock.

4. Conclusions and future considerations

The three pelagic *Sargassum* morphotypes investigated in this study present differences in their biochemical and elemental composition. This might be related to different source regions and dispersal patterns for SnI, SnVIII, and Sf, as recently suggested (Govindarajan et al., 2019). This will affect the properties of the *Sargassum* feedstock depending on the predominant morphotype during inundation events. Composition may also vary with the season and after storage of the collected biomass. Char

produced by pyrolysis can potentially be used as a soil enhancer. However, high concentrations of toxic arsenic may hamper this application. Accumulation of this metalloid in high concentrations can also render the pelagic *Sargassum* unusable for nutritional purposes, despite the presence of phlorotannins which have dietary and health benefits. In addition, *S. natans* and *S. fluitans* may not be suitable as a viable source of commercial alginates because yields of extraction are low compared to those of brown algae currently used for industrial production of alginate. However, both species may represent an interesting source of carbohydrates for microbial production of ethanol and bioplastics. Further investigation will help to define the best routes for exploitation of pelagic *Sargassum* harvested after inundation events. Valorisation of this seaweed biomass, informed by biological knowledge, will contribute to the sustainable management of the *Sargassum* crisis in the affected countries.

Acknowledgements

This project was supported through Research England's Quality Research Global Challenges Research Fund funding, awarded to the University of York. The authors wish to thank Paul Elliot for assistance with TGA samples, John Angus for ICP-MS analysis, and Glyn Hallam for technical support during collection of algal samples. The authors also thank Miss Nasheika Guyah for providing the picture of the Discovery Bay Marine Lab of the University of the West Indies - Mona (Jamaica) used in the graphical abstract.

Legends of figures

Figure 1. Sampling sites (A) and morphological identification (B) of *S. fluitans* and *S. natans* morphotypes. For *S. fluitans*, characteristic oblong to spherical air bladders with wings but without spines (A1), broad and medium length lanceolate blades with serrated edges (B1), and lateral branches with small spines (C1) were observed. For *S. natans* I, spherical air bladders without wings but with spines (A2), narrow and long linear blades with serrated edges (B2), and lateral branches with spines were present, except for Site C (C2). *S. natans* VIII featured spherical air bladders without wings and without spines (A3), broad and medium length to long lanceolate blades with serrated edges (B3), and lateral branches without spines (C3); presence of hydroid colonies (D3) was also observed.

Figure 2. TG plots of *S. natans* I (SnI), *S. fluitans* III (Sf), *S. natans* VIII (SnVIII), and bulk samples (Sfm) collected at three different sites (A, B, and C). Values in the inserted table corresponded to moisture, organic matter, calcium carbonate, and char content of each morphotype calculated by averaging data from weight loss curves obtained for the three sites of collection.

Figure 3. Monosaccharide composition in the non-cellulosic fraction of *S. natans* I (SnI), *S. fluitans* III (Sf), *S. natans* VIII (SnVIII), and bulk samples (Sfm).

Figure 4. Quantification of monosaccharides released by individual enzymatic treatments of *S. natans* I (SnI) site C, *S. fluitans* (Sf) site C, and *S. natans* VIII (SnVIII) site B. NE: no enzyme control; ED: enzyme digestion.

List of supplementary material

Supplementary Figure S1. Mass loss in *S. natans* I (SnI) site C, *S. fluitans* (Sf) site C, and *S. natans* VIII (SnVIII) site B samples estimated by preparation of alcohol insoluble residues (AIRs).

Supplementary Table S1. Moisture, organic matter, calcium carbonate, and char content in *S. natans* I (SnI), *S. fluitans* III (Sf), *S. natans* VIII (SnVIII), and bulk samples (Sfm) collected at three different sites (A, B, and C). Results are expressed in weight %.

Supplementary Table S2. Element composition analysis by ICP-MS of pelagic *Sargassum*. Results are expressed as µg/kg of biomass DW.

Supplementary Table S3. Determination of phenolic and phlorotannin contents in pelagic *Sargassum*. Results are expressed as mg/g of biomass DW.

Supplementary Table S4. Monosaccharide composition of pelagic *Sargassum*. Results are expressed as µg of monosaccharides/mg biomass DW.

Supplementary Table S5. Quantification of monosaccharides released after different enzymatic treatments of pelagic *Sargassum* biomass. Results are expressed as µg of monosaccharides/mg biomass DW.

References.

- Addico, G.N., deGraft-Johnson, K.A. 2016. Preliminary investigation into the chemical composition of the invasive brown seaweed *Sargassum* along the West Coast of Ghana. *Afr. J. Biotechnol.* 15, 2184-2191.
- Adet, L., Nsofor, G.N., Ogunjobi, K.O. and Camara, B. 2017. Knowledge of Climate Change and the Perception of Nigeria's Coastal Communities on the Occurrence of *Sargassum natans* and *Sargassum fluitans*. *OALib. J.*, 4: e4198.
- Ali, I., Bahadar, A. 2017. Red Sea seaweed (*Sargassum* spp.) pyrolysis and its devolatilization kinetics. *Algal Res.* 21, 89-97.
- Álvarez-Viñas, M., Flórez-Fernández, N., González-Muñoz, M.J., Domínguez, H. 2019. Influence of molecular weight on the properties of *Sargassum muticum* fucoidan. *Algal Res.* 38, 101393
- Amaral-Zettler, L.A., Dragone, N.B., Schell, J., Slikas, B., Murphy, L.G., Morrall, C.E., Zettler, E.R. 2017. Comparative mitochondrial and chloroplast genomics of a genetically distinct form of *Sargassum* contributing to recent "Golden Tides" in the Western Atlantic. *Ecol. Evol.* 7, 516-525.
- Anastasakis, K., Ross, A.B., Jones, J.M., 2011. Pyrolysis behaviour of the main carbohydrates of brown macro-algae. *Fuel* 90, 598-607.
- Azizi, N., Najafpour, G., Younesi, H. 2017. Acid pretreatment and enzymatic saccharification of brown seaweed for polyhydroxybutyrate (PHB) production using *Cupriavidus necator*. *Int. J. Biol. Macromol.* 101, 1029-1040.

516 Bae, Y.J., Ryu, C., Jeon, J.K. 2011. The characteristics of bio-oil produced from the pyrolysis of three
517 marine macroalgae. *Bioresour. Technol.* 102, 3512-3520.

518 Baker, P., Minzlaff, U., Schoenle, A., Schwabe, E., Hohlfeld, M., Jeuck, A., Brenke, N., Prausse, D.,
519 Rothenbeck, M., Brix, S., Frutos, I., Jörger, K.M., Neusser, T.P., Koppelman, R., Devey, C., Brandt,
520 A., Arndt, H. 2018. Potential contribution of surface-dwelling *Sargassum* algae to deep-sea
521 ecosystems in the southern North Atlantic. *Deep Sea Res. II* 148, 21–34.

522 Balboa, E.M., Moure, A., Domínguez, H. 2015. Valorization of *Sargassum muticum* biomass according
523 to the biorefinery concept. *Mar. Drugs*. 13, 3745-3760.

524 Bird, K.T., Benson, P.H. 1987. *Seaweed Cultivation for Renewable Resources*; Elsevier: Amsterdam,
525 The Netherlands.

526 Borines, M.G., de Leon, R.L., Cuello, J.L. 2013. Bioethanol production from the macroalgae *Sargassum*
527 spp, *Bioresour. Technol.* 138, 22-29.

528 Deniaud-Bouët, E., Kervarec, N., Michel, G., Kloareg, B., Tonon, T., Hervé, C. 2014. Chemical and
529 enzymatic fractionation of cell-walls from Fucales: insights into the structure of the extracellular
530 matrix of brown algae. *Ann. Bot.* 114, 1203-1216.

531 Fernández, F., Boluda, C.J., Olivera, J., Guillermo, L.A. 2017. Análisis elemental prospectivo de la
532 biomasa algal acumulada en las costas de la República Dominicana durante 2015. *Centro Azúcar*
533 44, 11-22.

534 Fernando, I.S., Kim, M., Son, K.T., Jeong, Y., Jeon, Y.J. 2016. Antioxidant activity of marine algal
535 polyphenolic compounds: A mechanistic approach. *J. Med. Food* 19, 615-628.

536 Ford, L., Theodoridou, K., Sheldrake, G.N., Walsh, P.J. 2019. A critical review of analytical methods
537 used for the chemical characterisation and quantification of phlorotannin compounds in brown
538 seaweeds. *Phytochem. Anal.* 30, 587-599.

539 Gong, Z., Lu, X., Ma, M., Watt, C., Le, X.C. 2002. Arsenic speciation analysis. *Talanta* 16, 77-96.

540 Gorham, J., Lewey, S.A., 1984. Seasonal changes in the chemical composition of *Sargassum muticum*.
541 *Mar. Biol.* 80, 103-107.

542 Govindarajan, A.F., Cooney, L., Whittaker, K., Bloch, D., Burdorf, R.M., Canning, S., Carter, C.,
543 Cellan, S.M., Eriksson, F.A.A., Freyer, H., Huston, G., Hutchinson, S., McKeegan, K., Malpani, M.,

544 Merkle-Raymond, A., Ouellette, K., Petersen-Rockney, R., Schultz, M., Siuda A.N.S. 2019. The
545 distribution and mitochondrial genotype of the hydroid *Aglaophenia latecarinata* is correlated with
546 its pelagic *Sargassum* substrate type in the tropical and subtropical western Atlantic Ocean. PeerJ
547 7:e7814.

548 Gouvêa, L.P., Assis, J., Gurgel, C.F.D., Serrão, E.A., Silveira, T.C.L., Santos, R., Duarte, C.M.; Peres,
549 L.M.C.; Carvalho, V.F.; Batista, M., Bastos, E., Sissini, M.N., Horta, P.A. 2020. Golden carbon of
550 *Sargassum* forests revealed as an opportunity for climate change mitigation. Sci. Total Environ. 729,
551 138745.

552 Johns, E.M., Lumpkin, R., Putman, N.F., Smith, R.H., Muller-Karger, F.E., Rueda-Roa, D.T., Hu, C.,
553 Wang, M., Brooks, M.T., Gramer, L.J., Werner, F.E. 2020. The establishment of a pelagic
554 *Sargassum* population in the tropical Atlantic: biological consequences of a basin-scale long
555 distance dispersal event. Prog. Oceanogr. 182, 102269.

556 Jones, L., Milne, J.L., Ashford, D., McQueen-Mason, S.J. 2003. Cell wall arabinan is essential for guard
557 cell function. Proc. Natl. Acad. Sci. USA 100, 11783-11788.

558 Kim, S.S., Ly, H.V., Kim, J., Choi, J.H., Woo, H.C. 2013. Thermogravimetric characteristics and
559 pyrolysis kinetics of alga *Sargassum* sp. biomass. Bioresour. Technol. 139, 242-248.

560 Kim, S.-S., Ly, H.V., Choi, G.-H., Kim, J., Woo, H.C. 2012. Pyrolysis characteristics and
561 kinetics of the alga *Saccharina japonica*. Bioresour. Technol. 123, 445-451.

562 Kraan, S. 2013. Mass-cultivation of carbohydrate rich macroalgae, a possible solution for sustainable
563 biofuel production. Mitig. Adapt. Strateg. Glob. Change 18, 27-46.

564 Langin, K. 2018. Seaweed masses assault Caribbean islands. Science 360, 1157-1158.

565 Lima, M.A., Gomez, L.D., Steele-King, C.G., Simister, R., Bernardinelli, O., Carvalho, M.A., Rezende,
566 C.A., Labate, C.A., de Azevedo, E.R., McQueen-Mason, S.J. 2014. Evaluating the composition and
567 processing potential of novel sources of Brazilian biomass for sustainable biorenewables production.
568 Biotechnol. Biofuels 7, 10.

569 Milledge, J.J., Harvey, P.J. 2016. Golden tides: Problem or golden opportunity? The valorisation of
570 *Sargassum* from beach inundations. J. Mar. Sci. Eng. 4, 60.

571 Milledge, J.J., Nielsen, B.V., Bailey, D. 2016. High-value products from macroalgae: the potential uses
572 of the invasive brown seaweed, *Sargassum muticum*. Rev. Environ. Sci. Biotechnol. 15, 67-88.

573 Milledge, J.J., Maneein, S., López, E.A., Bartlett, D. 2020. *Sargassum* Inundations in Turks and Caicos:
574 methane potential and proximate, ultimate, lipid, amino acid, metal and metalloid analyses.
575 Energies, 13, 1523.

576 Mohammed, A., Bissoon, R., Bajnath, E., Mohammed, K., Lee, T., Bissram, M., John, N., Jalsa, N.K.,
577 Lee, K.-Y., Ward, K. 2018. Multistage extraction and purification of waste *Sargassum natans* to
578 produce sodium alginate: An optimization approach. Carbohydr. Polym. 198, 109-118.

579 Mohammed, C., Mahabir, S., Mohammed K., John, N., Lee, K.-Y., Ward, K. 2019. Calcium alginate
580 thin films derived from *Sargassum natans* for the selective adsorption of Cd²⁺, Cu²⁺, and Pb²⁺ ions.
581 Ind. Eng. Chem. Res. 58, 1417-1425.

582 Ody, A., Thibaut T., Berline, L., Changeux, T., André, J.-M., Chevalier, C., Blanfuné, A., Blanchot, J.,
583 Ruitton, S., Stiger-Pouvreau, V., Connan, S., Grelet, J., Aurelle, D., Guéné, M., Bataille, H.,
584 Bachelier, C., Guillemain, D., Schmidt, N., Fauvelle, V., Guasco, S., Ménard F. 2019. From In Situ
585 to satellite observations of pelagic *Sargassum* distribution and aggregation in the Tropical North
586 Atlantic Ocean. PLoS ONE 14, e0222584.

587 Official Journal of the European Union, 2019. Commission Regulation (EU) 2019/1869 of 7 November
588 2019 amending and correcting Annex I to Directive 2002/32/EC of the European Parliament and of
589 the Council as regards maximum levels for certain undesirable substances in animal feed. Available
590 at <https://eur-lex.europa.eu/legal-content/EN/TXT/PDF/?uri=CELEX:32019R1869&from=EN>.

591 Ofori, O.O., Rouleay, M.D. 2020. Willingness to pay for invasive seaweed management: Understanding
592 how high and low income households differ in Ghana. Ocean Coast. Manag. 192, 105224.

593 Oviatt, C.A., Huizenga, K., Rogers, C.S., Miller, W.J. 2019. What nutrient sources support anomalous
594 growth and the recent *Sargassum* mass stranding on Caribbean beaches? A review. Mar. Pollut. Bull.
595 145, 517-525.

596 Oyesiku, O.O., Egunyomi, A. 2014. Identification and chemical studies of pelagic masses of *Sargassum*
597 *natans* (Linnaeus) Gaillon and *S. fluitans* (Borgessen) Borgesen (brown algae), found offshore in
598 Ondo State, Nigeria. Afr. J. Biotechnol. 13, 1188-1193.

- Pérez-Larrán, P., Torres, M.D., Flórez-Fernández, N., Balboa, E.M., Moure, A., Domínguez, H. 2019. Green technologies for cascade extraction of *Sargassum muticum* bioactives. J. Appl. Phycol. 31, 2481-2495.
- Peteiro, C. 2018. Alginate production from marine macroalgae, with emphasis on kelp farming. Springer Ser. Biomater. Sci. Eng. 11, 27-66.
- Plouguerné, E., Le Lann, K., Connan, S., Jechoux, G., Deslandes, E., Stiger-Pouvreau, V. 2006. Spatial and seasonal variation in density, reproductive status, length and phenolic content of the invasive brown macroalga *Sargassum muticum* (Yendo) Fensholt along the coast of western Brittany (France). Aquat. Bot. 85, 337-344.
- Putman, N.F., Goni, G.J., Gramer, L.J., Hu, C., Johns, E.M, Trinanés, J., Wang, M. 2018. Simulating transport pathways of pelagic *Sargassum* from the Equatorial Atlantic into the Caribbean Sea. Prog. Oceanog. 165, 205-214.
- Resiere, D., Valentino, R., Nevière, R., Banydeen, R., Gueye, P., Florentin, J., Cabié, A., Lebrun, T., Mégarbane, B., Guerrier, G., Mehdaoui, H. 2018. *Sargassum* seaweed on Caribbean islands: An international public health concern. Lancet 392, 2691.
- Rhein-Knudsen, N., Ale, M.T., Ajallouéian, F., Meyer, A.S. 2017. Characterization of alginates from Ghanaian brown seaweeds: *Sargassum* spp. and *Padina* spp. Food Hydrocoll. 71, 236-244.
- Roberts, D.A., Paul, N.A., Dworjanyn, S.A., Bird, M.I., de Nys, R. 2015. Biochar from commercially cultivated seaweed for soil amelioration. Sci. Rep. 5, 9665.
- Rodríguez-Martínez, R.E., Roy, P.D., Torrescano-Valle, N., Cabanillas-Terán, N., Carrillo-Domínguez, S., Collado-Vides, L., García-Sánchez, M., van Tussenbroek, B.I. 2020. Element concentrations in pelagic *Sargassum* along the Mexican Caribbean coast in 2018-2019. PeerJ 8, e8667.
- Rosado-Espinosa, L.A., Freile-Peigrín, Y., Hernández-Nuñez, E., Robledo, D. 2020. A comparative study of *Sargassum* species from the Yucatan Peninsula coast: morphological and chemical characterisation. Phycologia, 59:3, 261-271.
- Ross, A.B., Anastasakis, K., Kubacki, M.L., Jones, J.M. 2009. Investigation of the pyrolysis behaviour of brown algae before and after pre-treatment using PY-GC/MS and TGA. J. Anal. Appl. Pyrol. 85, 3-10.

627 Saldarriaga-Hernandez, S., Hernandez-Vargas, G., Iqbal, H.M.N., Barceló, D., Parra-Saldívar, R. 2020.
628 Bioremediation potential of *Sargassum* sp. biomass to tackle pollution in coastal ecosystems:
629 Circular economy approach. *Sci. Total Environ.* 715, 136978.

630 Schell, J.M., Goodwin, D.S., Siuda, A.N.S. 2015. Recent *Sargassum* inundation events in the
631 Caribbean. *Oceanography*, 28, 8-10.

632 Sembera, J.A., Meier, E.J., Waliczek, T.M. 2018. Composting as an alternative management strategy
633 for *Sargassum* drifts on coastlines. *Horttechnology* 28, 80-84.

634 Singleton, V.L., Orthofer, R., Lamuela-Raventós, R. 1999. Analysis of total phenols and other oxidation
635 substrates and antioxidants by means of Folin–Ciocalteu reagent. *Methods Enzymol.* 299, 152-178.

636 Smetacek, V., Zingone, A. 2013. Green and golden seaweed tides on the rise. *Nature* 504, 84-88.

637 Soliman, R.M., Younis, S.A., El-Gendy, N.S., Mostafa, S.S.M., El-Temtamy, S.A., Hashim, A.I. 2018.
638 Batch bioethanol production via the biological and chemical saccharification of some Egyptian
639 marine macroalgae. *J. Appl. Microbiol.* 125, 422-440.

640 Stern, J.L., Hagerman, A.E., Steinberg, P.D, Winter, F.C., Estes, J.A. 1996. A new assay for quantifying
641 brown algal phlorotannins and comparisons to previous methods. *J. Chem. Ecol.* 22, 1273-1293.

642 Taylor, P.D., Monks, N. 1997. A new cheilostome bryozoan genus pseudoplanktonic on molluscs and
643 algae. *Invertebr. Biol.* 116, 39-51.

644 Templeton, D.W., Wolfrum, E.J., Yen, J.H., Sharpless, K.E. 2016. Compositional analysis of biomass
645 reference materials: results from an interlaboratory study. *Bioenerg. Res.* 9, 303-314.

646 Thompson, T.M, Young, B.R., Baroutian, S. 2020. Pelagic *Sargassum* for energy and fertiliser
647 production in the Caribbean: A case study on Barbados. *Renew. Sust. Energ. Rev.* 118, 109564.

648 Weis, J.S., (1968). Fauna associated with pelagic *Sargassum* in the Gulf Stream. *Am. Midl. Nat.* 80,
649 554-558.

650 Wang, M, Hu C, Barnes, BB, Mitchum, G, Lapointe, B, Montoya J.P. 2019. The great Atlantic
651 *Sargassum* belt. *Science* 365, 83-87.

652 Zubia, M., Payri, C., Deslandes, E. 2008. Alginate, mannitol, phenolic compounds and biological
653 activities of two range-extending brown algae, *Sargassum mangarevense* and *Turbinaria ornata*
654 (Phaeophyta: Fucales), from Tahiti (French Polynesia). *J. Appl. Phycol.* 20, 1033-1043.

Table 1. Element contents determined by ICP-MS in pelagic morphotypes *S. natans* I (SnI), *S. natans* VIII (SnVIII), and *S. fluitans* III (Sf) collected at site A. Results (mean \pm SD) are expressed as $\mu\text{g/g}$ of biomass DW.

Elements	SnI	SnVIII	Sf
Na	11,441.00 \pm 237.24	14,436.18 \pm 575.76	11,310.71 \pm 406.27
Mg	8,456.26 \pm 300.36	6,193.47 \pm 146.48	8,684.03 \pm 292.54
Al	335.69 \pm 18.70	187.70 \pm 31.79	427.57 \pm 54.94
K	28,701.30 \pm 527.46	32,865.84 \pm 1003.03	30,503.78 \pm 1225.51
Ca	56,138.23 \pm 1864.90	36,435.64 \pm 690.72	57,726.79 \pm 1813.97
V	2.37 \pm 0.06	2.28 \pm 0.18	4.21 \pm 0.43
Cr	3.18 \pm 0.99	1.50 \pm 0.54	9.18 \pm 0.37
Mn	39.62 \pm 0.36	13.03 \pm 0.48	22.92 \pm 0.66
Fe	634.79 \pm 18.18	237.07 \pm 44.26	832.97 \pm 101.84
Co	0.91 \pm 0.07	0.47 \pm 0.03	0.89 \pm 0.06
Ni	4.21 \pm 0.16	3.87 \pm 0.10	3.52 \pm 0.08
Cu	4.29 \pm 0.16	2.78 \pm 0.14	4.47 \pm 0.20
Zn	14.71 \pm 1.98	6.35 \pm 0.62	7.2 \pm 1.20
As	64.91 \pm 0.61	60.30 \pm 0.34	58.32 \pm 2.29
Cd	0.77 \pm 0.43	0.40 \pm 0.02	0.57 \pm 0.02
Ba	22.17 \pm 0.67	19.21 \pm 0.65	23.21 \pm 0.42
Pb	2.47 \pm 1.79	0.33 \pm 0.13	1.11 \pm 0.47
U	0.80 \pm 0.08	0.79 \pm 0.01	0.83 \pm 0.04
Total	105,867.69 \pm 2926.44	90,467.20 \pm 2410.74	109,622.32 \pm 3618.09

Table 2. Determination of the phenolic (FC method) and phlorotannin (DMBA method) contents in pelagic morphotypes *S. natans* I (SnI), *S. natans* VIII (SnVIII), *S. fluitans* III (Sf), and in the bulk samples (Sfm). Results (mean \pm SD) are expressed as mg PGE/g of biomass DW.

	SnI	SnVIII	Sf	Sfm
FC	2.13 \pm 0.46	3.11 \pm 0.74	1.20 \pm 0.43	1.42 \pm 0.48
DMBA	0.62 \pm 0.11	0.91 \pm 0.32	0.39 \pm 0.21	0.34 \pm 0.14

Table 3. Alginate content (mean \pm SD), determined by quantification of mannuronic (M) and guluronic (G) acid monomers, in pelagic morphotypes *S. natans* I (SnI), *S. natans* VIII (SnVIII), *S. fluitans* III (Sf), and in the bulk samples (Sfm).

Samples	Alginate (% dry weight)	Alginate (% total monosaccharides)	M (% alginate)	G (% alginate)	M/G ratio
SnI	11.13 \pm 2.02	66.85 \pm 2.45	65.05 \pm 1.47	34.95 \pm 1.47	1.87 \pm 0.12
SnVIII	12.18 \pm 2.10	66.09 \pm 2.59	65.86 \pm 3.58	34.14 \pm 3.58	1.97 \pm 0.39
Sf	9.36 \pm 2.51	65.15 \pm 4.83	65.49 \pm 3.80	34.51 \pm 3.80	1.94 \pm 0.42
Sfm	13.50 \pm 4.61	68.51 \pm 4.29	64.61 \pm 1.47	35.39 \pm 1.47	1.83 \pm 0.11

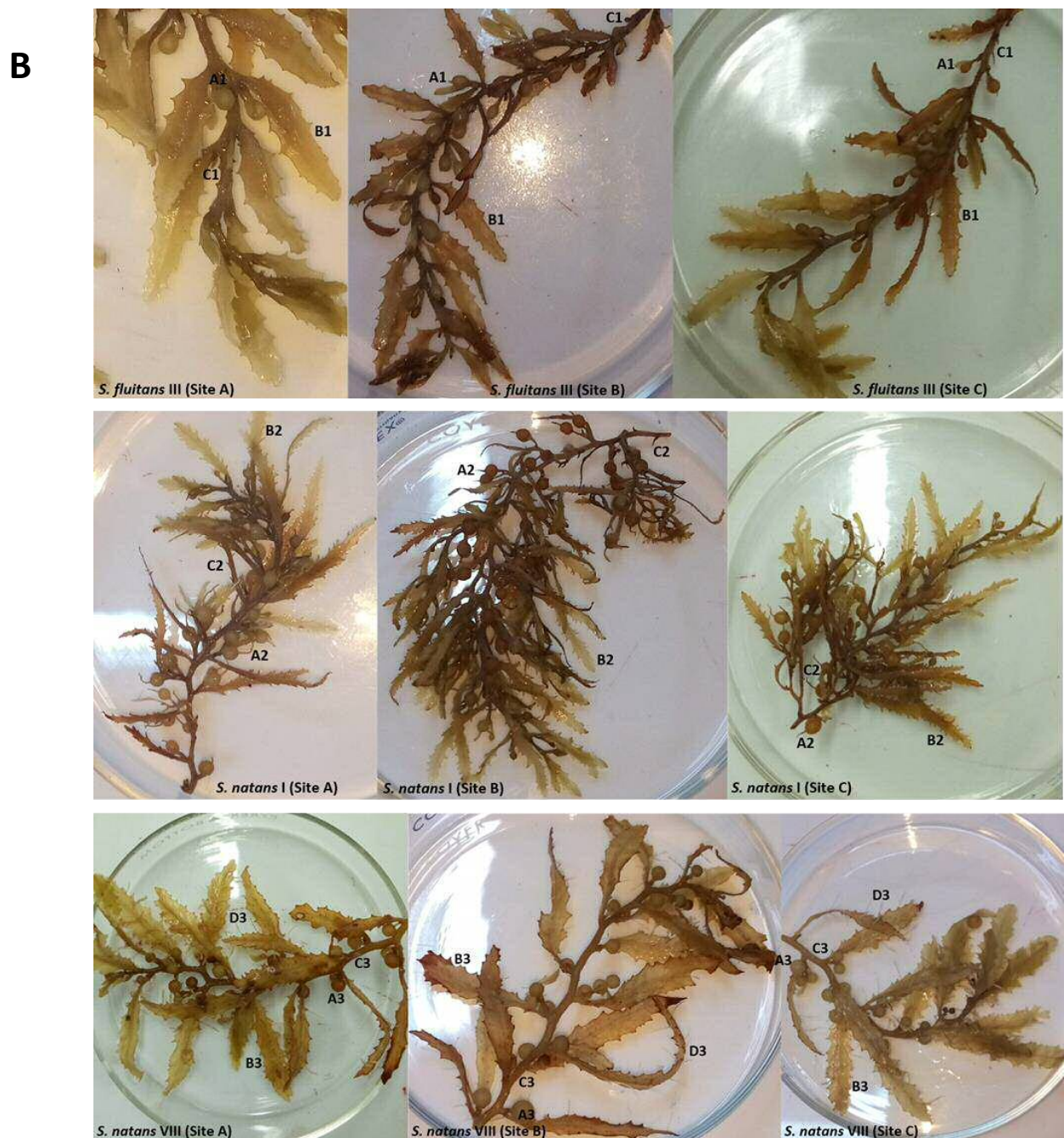


Figure 1. Sampling sites (A) and morphological identification (B) of *S. fluitans* and *S. natans* morphotypes. For *S. fluitans*, characteristic oblong to spherical air bladders with wings but without spines (A1), broad and medium length lanceolate blades with serrated edges (B1), and lateral branches with small spines (C1) were observed. For *S. natans* I, spherical air bladders without wings but with spines (A2), narrow and long linear blades with serrated edges (B2), and lateral branches with spines were present, except for Site C (C2). *S. natans* VIII featured spherical air bladders without wings and without spines (A3), broad and medium length to long lanceolate blades with serrated edges (B3), and lateral branches without spines (C3); presence of hydroid colonies (D3) was also observed.

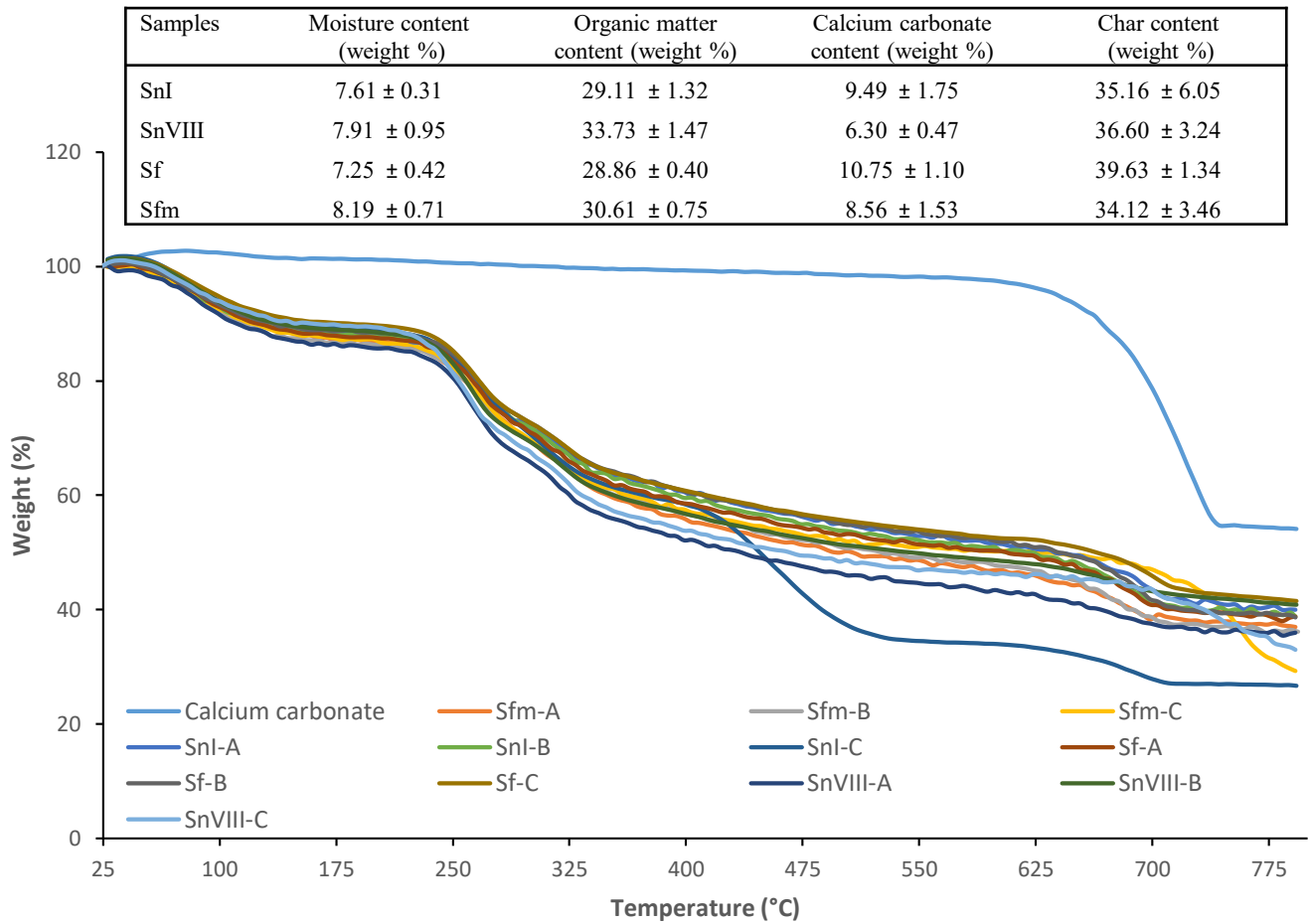


Figure 2. TG plots of *S. natans* I (SnI), *S. fluitans* III (Sf), *S. natans* VIII (SnVIII), and bulk samples (Sfm) collected at three different sites (A, B, and C). Values in the inserted table corresponded to moisture, organic matter, calcium carbonate, and char content of each morphotype calculated by averaging data from weight loss curves obtained for the three sites of collection.

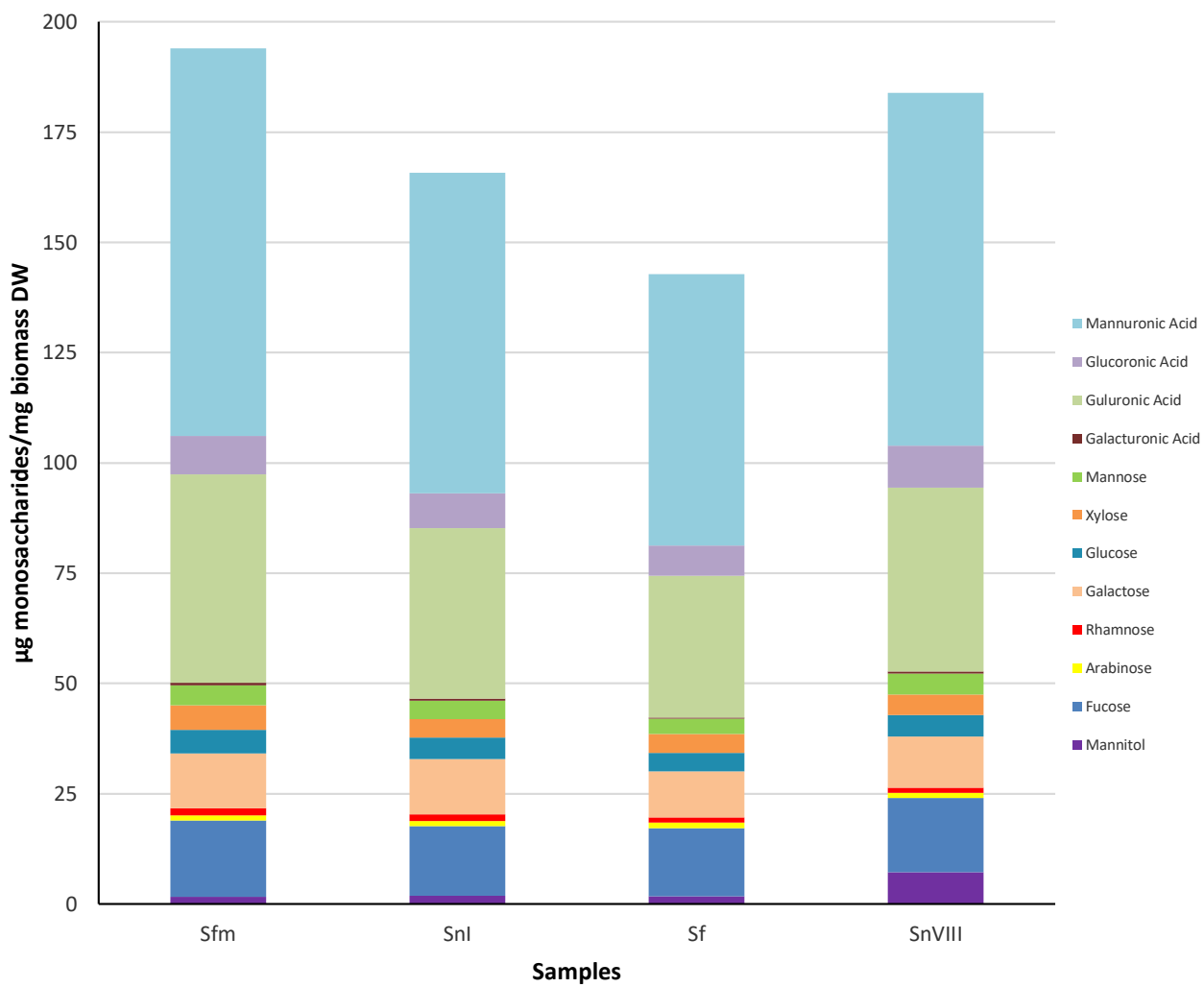


Figure 3. Monosaccharide composition in the non-cellulosic fraction of *S. natans* I (SnI), *S. fluitans* III (Sf), *S. natans* VIII (SnVIII), and bulk samples (Sfm).

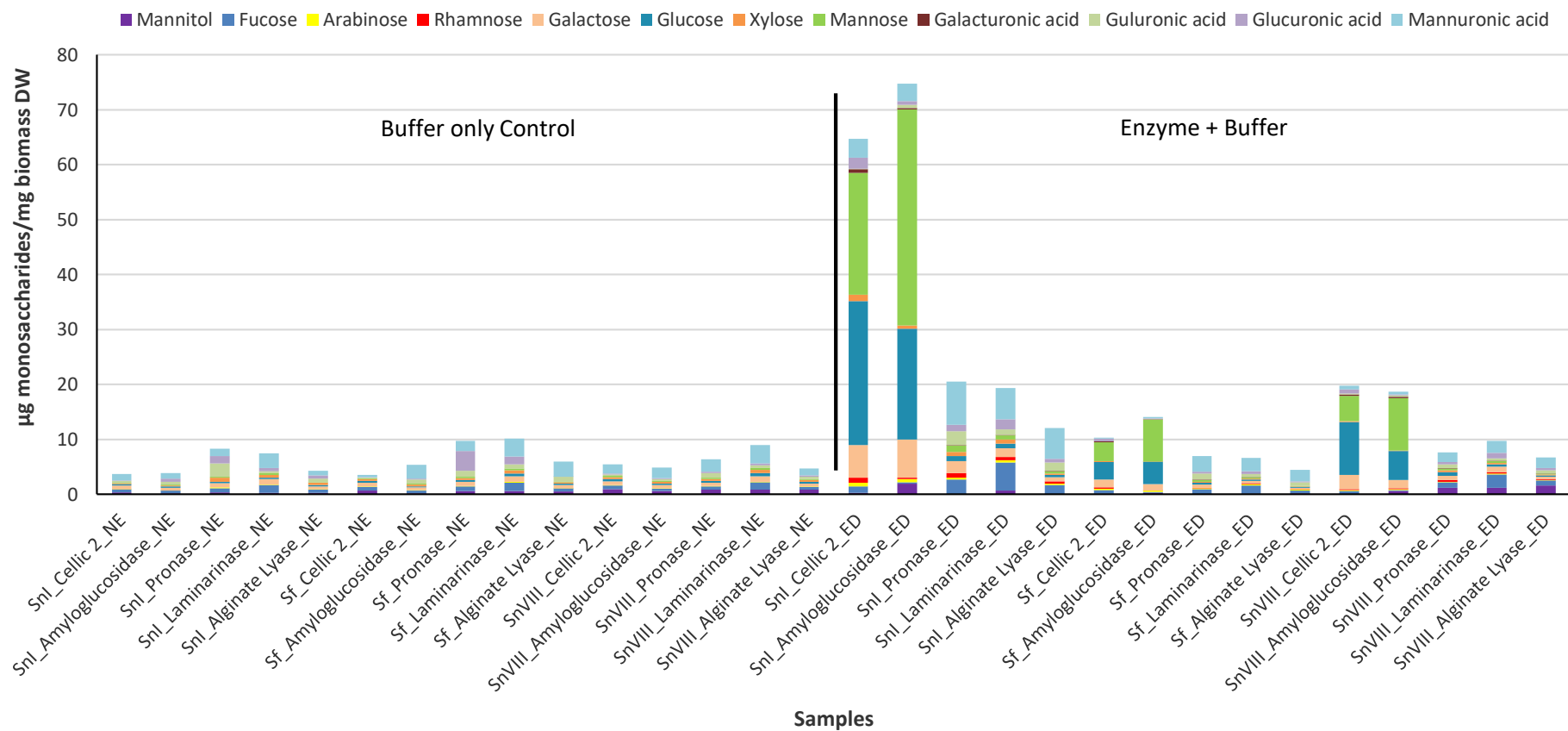


Figure 4. Quantification of monosaccharides released by individual enzymatic treatments of *S. natans* I (SnI) site C, *S. fluitans* (Sf) site C, and *S. natans* VIII (SnVIII) site B. NE: no enzyme control; ED: enzyme digestion.